

# B/C/N Materials and B<sub>4</sub>C Synthesized by a Non-Oxide Sol–Gel Process

Karl W. Völger,<sup>†</sup> Edwin Kroke,<sup>\*,†</sup> Christel Gervais,<sup>‡</sup> Tomohiro Saito,<sup>§</sup>  
Florence Babonneau,<sup>‡</sup> Ralf Riedel,<sup>†</sup> Yuji Iwamoto,<sup>§</sup> and Tsukasa Hirayama<sup>§</sup>

Department of Materials and Earth Science, Darmstadt University of Technology,  
Petersenstrasse 23, 64287 Darmstadt, Germany, Université Pierre et Marie Curie,  
Paris, France, and Japan Fine Ceramics Center, Nagoya, Japan

Received September 23, 2002. Revised Manuscript Received November 22, 2002

*B*-trichloroborazene B<sub>3</sub>N<sub>3</sub>H<sub>3</sub>Cl<sub>3</sub> reacts with bis(trimethylsilyl)carbodiimide Me<sub>3</sub>Si–NCN–SiMe<sub>3</sub> in THF or toluene, or without any solvent, to form non-oxide gels. The xerogels, amorphous B/C/N materials, and (semi)crystalline pyrolysis products were characterized using infrared (FTIR) and Raman spectroscopy, <sup>11</sup>B- and <sup>15</sup>N-nuclear magnetic resonance spectroscopy (NMR), X-ray powder diffraction (XRD), scanning electron microscopy (SEM), transmission electron microscopy (TEM), and elemental analysis. In addition, the pyrolysis process was investigated through thermal gravimetry coupled with mass spectrometry (TG–MS). The xerogels consist of a three-dimensional polymeric network of borazene rings linked by carbodiimide groups. Interestingly, the sol–gel transition is phenomenologically analogous to oxide systems and the polymers are almost free of chlorine and trimethylsilyl endgroups. Pyrolysis at 1200 °C provides an amorphous ceramic with the composition BC<sub>0.23</sub>N<sub>1.1</sub>Si<sub>0.05</sub>H<sub>0.09</sub> ≈ B<sub>4</sub>CN<sub>4</sub>. This material starts to crystallize around 1600 °C under evolution of nitrogen, forming nearly pure B<sub>4</sub>C at 2000 °C. Very small amounts of amorphous carbon as well as carbon nanotubes were also present.

## Introduction

Materials in the B/C/N system are of interest for several reasons. Novel graphitic ternary phases of these elements may possess properties intermediate between graphite and *h*-BN.<sup>1</sup> This might lead to enhanced oxidation (or corrosion) resistance or to tailorable (opto)-electronic properties. On the other hand, diamond and *c*-BN are known for their extreme hardness as well as other useful chemical and physical properties.<sup>2</sup> Besides, B<sub>4</sub>C is one of the hardest materials with diamond-like mechanical properties, and is already used for a variety of applications including armor plating, blasting nozzles, and mechanical seal faces, as well as for grinding and cutting tools. It is produced on an industrial scale by classical carbothermal reduction of B<sub>2</sub>O<sub>3</sub> in electric arc furnaces. Dense materials are obtained either by pressureless sintering or hot pressing at 2100–2250 °C. Typical methods to synthesize B/C/N materials include (carbo)nitridation of oxide starting materials, pyrolysis of solid and liquid precursors, high-temperature and high-pressure techniques, as well as CVD and PVD routes.<sup>3</sup>

In contrast, the classical sol–gel process based on hydrolysis reactions of alkoxides or halides is known as a synthesis method for oxide glasses and ceramics.<sup>4</sup>

Only a very few non-oxide sol–gel systems are known.<sup>5</sup> Recently Bradley et al. reported the first example of a sol–gel process based on an ammonolysis reaction. Si/(C)/N gels were prepared from a dialkylamino substituted cyclic trisilane.<sup>6</sup>

To our knowledge, there has been only one sol–gel route described in the literature which may be used to prepare B/C/N materials.<sup>7</sup> In the late 1980s Paine and Narula et al. synthesized *h*-BN and ternary B/C/N ceramics using “silazanalysis” reactions of *B*-trichloroborazene and its alkyl substituted derivatives with hexa- and heptamethyl disilazane. A three-dimensional network infiltrated with liquid Me<sub>3</sub>SiCl is formed which is analogous to the oxide polymer networks infiltrated by solvents and liquid reaction products. The dried xerogels showed low specific surface areas (<35 m<sup>2</sup>/g) compared to oxide xerogels. Pyrolysis at 1200 °C gave hexagonal boron nitride.<sup>7</sup> The crystallization behavior and the oxidation resistance of the products were investigated.<sup>8</sup> The process was used to coat metal oxide substrates with *h*-BN coatings.<sup>9</sup> Molecular model com-

(4) Brinker, C. J.; Scherer, G. W. *Sol–Gel Science*; Academic Press: San Diego, CA, 1990.

(5) Kroke, E. *Novel Sol–Gel Routes to Non-Oxide Ceramics*; In Proceedings of the 9th CIMTEC – World Ceramics Congress, Ceramics: Getting into the 2000's – Part C; Vincenzini, P., Ed.; Elsevier: New York, 1999; p 123.

(6) Rovai, R.; Lehmann, C. W.; Bradley, J. S. *Angew. Chem., Int. Ed.* **1999**, *38*, 2036. (b) Farrusseng, D.; Schlichte, K.; Spliethoff, B.; Wingen, A.; Kaskel, S.; Bradley, J. S.; Schuth, F. *Angew. Chem., Int. Ed.* **2001**, *40*, 4204.

(7) Narula, C. K.; Schaeffer, R.; Datye, A.; Paine, R. T. *Inorg. Chem.* **1989**, *28*, 4053.

(8) Narula, C. K.; Schaeffer, R.; Datye, A.; Borek, T. T.; Rapko, B. M.; Paine, R. T. *Chem. Mater.* **1990**, *2*, 384.

\* Corresponding author. E-mail: kroke@tu-darmstadt.de.

<sup>†</sup> Darmstadt University of Technology.

<sup>‡</sup> Université Pierre et Marie Curie.

<sup>§</sup> Japan Fine Ceramics Center.

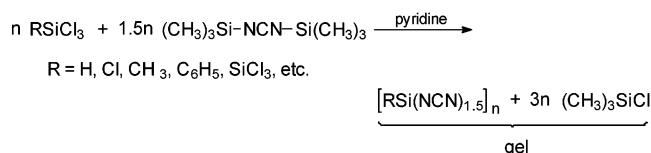
(1) Kawaguchi, M. *Adv. Mater.* **1997**, *8*, 615.

(2) Riedel, R. *Adv. Mater.* **1994**, *6*, 549.

(3) Overview: Weimer, A. W. *Carbide, Nitride and Boride Materials*; Chapman & Hall: New York, 1997.

pounds were synthesized and structurally characterized in order to examine the polymer structure of the gels.<sup>10</sup> Supercritical drying yielded B/C/N-aerogels.<sup>11</sup> The results concerning this sol-gel process and its application to synthesize B(C)/N-ceramics were summarized in a comprehensive review article and compared with classical routes to boron nitride.<sup>12</sup> According to our knowledge, all other attempts to obtain boron carbonitrides by sol-gel approaches such as ammonolysis or aminolysis of borazene halides or reactions of BCl<sub>3</sub> with silazanes (e.g., HMDS) have failed. Similarly, for carbides, nitrides, and carbonitrides of other elements, as well as further non-oxide materials such as sulfides, selenides, and borides, etc., there are only very few examples of sol-gel processes known. Most attempts to synthesize non-oxide gels resulted in the formation of dense, solid precipitates.<sup>5</sup>

Our approach to synthesize polymer and gel precursors for carbide and nitride materials is based on the pseudo-chalcogen concept which was developed by Koehler et al. in the 1970s and 1980s.<sup>13</sup> Instead of using silazanes<sup>14</sup> and carbosilanes<sup>15</sup> for the synthesis of Si(C)/N and SiC ceramics, we replaced the oxygen atoms in polysiloxanes by carbodiimide (–N=C=N–) groups in order to obtain (poly)silylcarbodiimide compounds.<sup>16</sup> Dichlorosilanes such as (CH<sub>3</sub>)<sub>2</sub>SiCl<sub>2</sub> form linear and cyclic oligomers upon polycondensation reactions with cyanamide H<sub>2</sub>N–CN or bis(trimethylsilyl)carbodiimide (CH<sub>3</sub>)<sub>3</sub>Si–NCN–Si(CH<sub>3</sub>)<sub>3</sub>. It was found that methyltrichlorosilane reacts with bis(trimethylsilyl)carbodiimide (BTSC) to form transparent gels.<sup>17</sup> Later, it turned out that almost all trichlorosilanes (RSiCl<sub>3</sub> with R = alkyl, aryl, or H), as well as tetrachlorosilane and some dichlorosilanes, react similarly with BTSC.<sup>5,16,18</sup>



The changes of rheological properties during the sol-gel transition are qualitatively and even quantitatively

(9) Paine, R. T.; Narula, C. K.; Schaeffer, R.; Datye, A. *Chem. Mater.* **1989**, *1*, 486. (b) Borek, T. T.; Qui, X.; Rayfuse, L. M.; Datye, A.; Paine, R. T.; Allard, L. F. *J. Am. Ceram. Soc.* **1991**, *74*, 2587.

(10) Narula, C. K.; Lindquist, D. A.; Fan, M.-M.; Borek, T. T.; Duesler, E. N.; Datye, A. K.; Schaeffer, R.; Paine, R. T. *Chem. Mater.* **1990**, *2*, 377.

(11) Lindquist, D. A.; Borek, T. T.; Kramer, S. J.; Narula, C. K.; Johnston, G.; Schaeffer, R.; Smith, D. M.; Paine, R. T. *J. Am. Ceram. Soc.* **1990**, *73*, 757.

(12) Paine, R. T.; Narula, C. K. *Chem. Rev.* **1990**, *90*, 73.

(13) Overview: Jäger, L.; Köhler, H. *Sulfur Reports* **1992**, *12*, 159.

(14) Overview: Kroke, E.; Li, Y.-L.; Konetschny, C.; Lecomte, E.; Fasel, C.; Riedel, R. *Mater. Sci. Eng. R* **2000**, *26*, 97.

(15) Overviews: (a) Narula, C. K. *Ceramic Precursor Technology and its Applications*; Marcel Dekker Inc.: New York, 1995. (b) Birot, M.; Pillot, J.-P. *Chem. Rev.* **1995**, *95*, 1443.

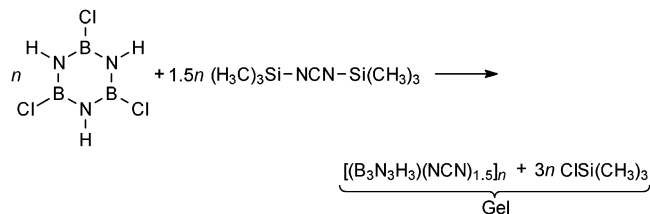
(16) Overview: Riedel, R.; Kroke, E.; Greiner, A.; Gabriel, A. O.; Ruwisch, L.; Nicolich, J.; Kroll, P. *Chem. Mater.* **1998**, *10*, 2964.

(17) Gabriel, A. O.; Riedel, R. *Angew. Chem.* **1997**, *109*, 371; *Angew. Chem., Int. Ed. Engl.* **1997**, *36*, 384. (b) Gabriel, A. O.; Riedel, R.; Storck, S.; Maier, W. F. *Appl. Organomet. Chem.* **1997**, *11*, 833. (c) Gabriel, A. O.; Riedel, R.; Dressler, W.; Reichert, S.; Gervais, C.; Maquet, J.; Babonneau, F. *Chem. Mater.* **1999**, *11*, 412.

(18) Kroke, E.; Gabriel, A. O.; Kim, D. S.; Riedel, R. *Organosilicon Chemistry IV*; Auner, N., Weis, J. Eds.; Wiley-VCH: Weinheim, 2000; p 812. (b) Kim, D. S.; Kroke, E.; Riedel, R.; Gabriel, A. O.; Shim, S. C. *Appl. Organomet. Chem.* **1999**, *13*, 495. (c) Völger, K. W. Diploma Thesis, Technische Universität Darmstadt, Germany, 1998 (in German).

very similar to those of oxide sol-gel systems.<sup>19</sup> It was possible to generate spherical, monodisperse, silicon dicarbodiimide particles analogous to the Stöber process which is known as a synthetic route to spherical oxide particles.<sup>20</sup> The crystallization behavior of polysilylcarbodiimides was investigated and compared to that of silazane derived materials.<sup>21</sup> Ceramic Si/C/N membranes were fabricated and tested for their gas separation properties.<sup>22</sup>

In a recently published communication we reported on a novel sol-gel route to B<sub>4</sub>C.<sup>23</sup> *B*-trichloroborazene (B<sub>3</sub>N<sub>3</sub>H<sub>3</sub>Cl<sub>3</sub>) reacts with BTSC in THF or toluene or even without any solvent to form non-oxide gels.



The xerogels obtained after aging and drying were practically free of any chlorine or oxygen and contained only small amounts of silicon. At 1200 °C an amorphous B/C/N material with a composition very close to B<sub>4</sub>CN<sub>4</sub> was obtained. Around 1800 °C this material evolved nitrogen and crystallized to form pure B<sub>4</sub>C. Here we present the results of a detailed investigation of this pyrolysis and crystallization process using XRD, TEM, SEM, FTIR, Raman, solid-state <sup>11</sup>B NMR and <sup>15</sup>N NMR spectroscopy, as well as nitrogen absorption measurements (BET), elemental analysis, and TG-MS.

## 2. Experimental Section

**Synthesis of Gels and Ceramic Materials.** All manipulations were performed under inert atmosphere using a glovebox and/or Schlenk techniques. *B*-trichloroborazene<sup>24</sup> and bis(trimethylsilyl)carbodiimide (BTSC)<sup>25</sup> were synthesized according to the literature as follows. BTSC was prepared from a mixture of hexamethyldisilazane, cyanoguanidine, and a catalytic amount of ammonium sulfate by heating to reflux for 8 h and distillation over a Vigreux column at 164 °C. *B*-trichloroborazene was obtained from a reaction of hexamethyldisilazane and boron trichloride and purified by sublimation in a vacuum at 60 °C. Toluene and THF were dried with a sodium-benzophenone mixture under reflux. Details of the gel synthesis were described recently.<sup>23</sup> In a typical experiment 5 g of *B*-trichloroborazene was dissolved in 10 mL of dry THF/toluene or directly in an excess of BTSC. To decrease the gelation time the liquid homogeneous mixtures were heated to 45 °C or to the boiling point. Depending on the temperature, gelation was observed within 0.5 and 100 h. After an aging period of 2–40 days the gels were carefully dried in a vacuum at 150 °C. In most cases the products consisted of

(19) Balan, C.; Völger, K. W.; Kroke, E.; Riedel, R. *Macromolecules* **2000**, *33*, 3404.

(20) Li, Y.-L.; Kroke, E.; Klonezyski, A.; Riedel, R. *Adv. Mater.* **2000**, *12*, 956.

(21) Iwamoto, Y.; Völger, K. W.; Kroke, E.; Riedel, R.; Saitou, T.; Matsunaga, K. *J. Am. Ceram. Soc.* **2001**, *84*, 2170.

(22) Völger, K. W.; Iwamoto, Y.; Kroke, E.; Riedel, R. *Materials Week 2002 – Proceedings*; Werkstoffwoche-Partnerschaft GbRmbH: Frankfurt, Germany, in press.

(23) Kroke, E.; Völger, K. W.; Klonezyski, A.; Riedel, R. *Angew. Chem.* **2001**, *113*, 1751, *Angew. Chem., Int. Ed.* **2001**, *40*, 1698.

(24) Nöth, H.; Sachdev, H. *Z. Naturforschung* **1997**, *52 b*, 1345.

(25) Vostokov, I. A.; Dergunov, Y. I. *Zh. Obshch. Khim.* **1977**, *47*, 1769.

**Table 1. Elemental Analyses Results of the Xerogel and the Amorphous and Crystalline Pyrolysis Products**

product	B	C	N	Si mass%	H	O	Cl	Σ	molecular formula
xerogel (150 °C/10 <sup>-2</sup> Torr/1h)	19.5	19.1	49.5	5.4	3.8	1.2	0.3	98.8	BC <sub>0.88</sub> N <sub>1.96</sub> Si <sub>0.11</sub> H <sub>2.09</sub> O <sub>0.04</sub> (~BCN <sub>2</sub> H <sub>2</sub> )
amorphous product (1200 °C/Ar/2h)	34.9	8.9	49.7	4.7	< 0.3	1.8	< 0.1	< 100.4	BC <sub>0.23</sub> N <sub>1.1</sub> Si <sub>0.05</sub> H <sub>0.09</sub> O <sub>0.03</sub> (~B <sub>4</sub> CN <sub>4</sub> )
crystalline product (2000 °C/He/4h)	78.3	21.0	n.d. <sup>a</sup>	n.d. <sup>a</sup>	n.d. <sup>a</sup>	n.d. <sup>a</sup>	n.d. <sup>a</sup>	99.3	BC <sub>0.24</sub> (B <sub>4</sub> C <sub>0.97</sub> ) (~B <sub>4</sub> C)

<sup>a</sup> n.d. = not determined.

white, air-sensitive powders. Sometimes bulk xerogel bodies were obtained.

Pyrolysis of the xerogels was performed in quartz-Schlenk tubes under flowing argon at 400, 600, 800, 1000, and 1200 °C for 2 h using a heating rate of 100 K/h in a tube furnace (model 56-500/788, Gero Co., Neuhausen, Germany). Before heat treatment, the xerogels were ground to a fine powder using a mortar and pestle. Further annealing at 1600 and 1800 °C in Ar and at 2000 °C in He was performed in a graphite furnace (Astro 1000-4560-FP20, Thermal Technology Inc., Santa Rosa, CA) with graphite crucibles. Heating rates of 600 K/h up to 1200 °C followed by 300 K/h and holding times of 4 h were applied.

**Methods of Characterization.** All manipulations of gels, xerogels, and pyrolysis products obtained below 1000 °C were performed under inert gas using glovebox and/or Schlenk techniques. FTIR spectra were recorded using the standard KBr pellet method and with a single reflection diamond crystal ATR unit (Perkin-Elmer PE 1750 spectrometer, Shelton, CT, and "Golden Gate" Mark II, L. O. T.-Oriol, Darmstadt, Germany). A Bruker IFS 55 spectrometer was used for the Raman measurements. X-ray powder diffraction patterns were obtained with a STOE STADI-P-diffractometer and on a Bragg–Brentano diffractometer Siemens D500 ( $\lambda = 1.5418 \text{ \AA}$ , Cu K $\alpha$ ). The xerogels and pyrolysis products were ground in a mortar and measured in reflection geometry using an acrylic glass sample holder.

The solid-state NMR spectra were recorded on a Bruker MSL 300 spectrometer operating at 30.41 MHz for <sup>15</sup>N and on a Bruker MSL 400 spectrometer at a frequency of 128.28 MHz using a Doty probe with no probe background for <sup>11</sup>B. Samples were spun at 5 kHz for the <sup>15</sup>N experiments, using 7-mm ZrO<sub>2</sub> rotors filled up in a glovebox under a dried argon atmosphere, whereas samples were spun at 10 kHz for the <sup>11</sup>B experiments using 5-mm ZrO<sub>2</sub> rotors filled up in a glovebox under dried argon atmosphere. All the <sup>15</sup>N CP and IRCP experiments were performed under the same Hartmann–Hahn match condition: both RF channel levels,  $\omega_{1S/2\tau}$  and  $\omega_{1I/2\tau}$ , were set about 42 kHz.

<sup>15</sup>N chemical shifts were referenced to solid NH<sub>4</sub>NO<sub>3</sub> (10% enriched sample,  $\delta_{\text{iso}}(^{15}\text{NO}_3) = -4.6 \text{ ppm}$  compared to CH<sub>3</sub>-NO<sub>2</sub> ( $\delta = 0 \text{ ppm}$ )), whereas <sup>11</sup>B chemical shifts were determined relative to liquid BF<sub>3</sub>OEt<sub>2</sub> ( $\delta = 0 \text{ ppm}$ ).

TG–MS was performed on a Netzsch STA 429 (Selb, Germany) coupled with a Balzers QMG 420 mass spectrometer using flowing helium (75 cm<sup>3</sup>/min) and a heating rate of 5 K/min. Nitrogen adsorption measurements (Quantachrome Autosorb-3B) were carried out after desorption at 180 °C/0.5 mbar for 12 h of samples (~0.5 g) which were ground in a mortar. SEM images were taken with a Phillips XL 30 FEG (Phillips Research Lab., Eindhoven, The Netherlands) using standard preparation techniques, i.e., carbon or gold coated powder samples. The microstructure of heat-treated samples was studied using a TEM (model EM-002B, Topcon Co., Tokyo, Japan, operating at 200 kV) equipped with an energy-dispersive X-ray (EDX) analysis system (model 9900, Philips Research Lab., Eindhoven, The Netherlands). The sample was prepared on a copper micromesh screen. Chemical analysis (B, Cl, Si, N, C, O, and H) was done at the Microanalytisches Labor Pascher, 53424 Remagen (Germany). All FTIR, Raman, and NMR spectra as well as the XRD patterns, TEM and SEM images, and SAED patterns were recorded at room temperature.

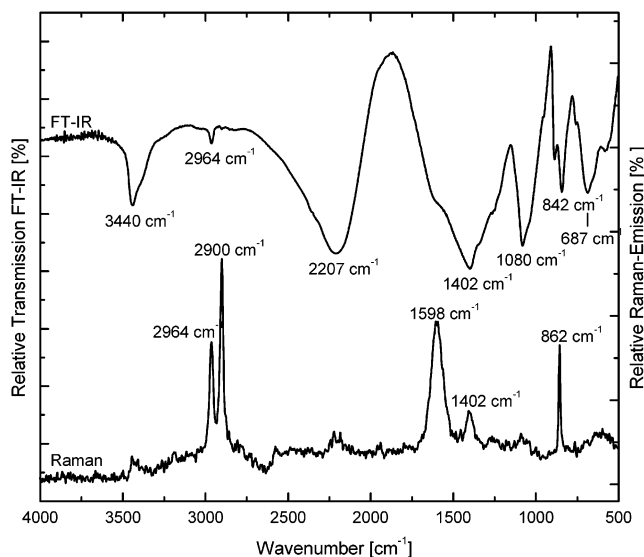
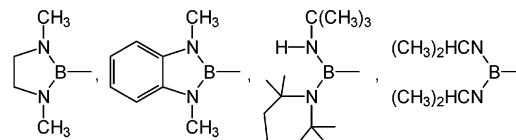
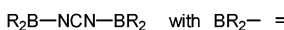


**Figure 1.** FT-IR and Raman spectra of the BCN<sub>2</sub>H<sub>2</sub> xerogel, dried in a vacuum at 150 °C.

### 3. Results and Discussion

**3.1 Synthesis and Structure of the Xerogels.** On the search for novel non-oxide sol–gel systems and ternary B/C/N phases we examined the reactions of BCl<sub>3</sub> and BF<sub>3</sub> with BTSC.<sup>26</sup> It turned out that solid, insoluble, and infusible products are formed, which contain either residual chlorine or significant amounts of silicon, depending on the reaction conditions. In contrast, we discovered that *B*-trichloroborazene (B<sub>3</sub>N<sub>3</sub>H<sub>3</sub>Cl<sub>3</sub>) reacts with BTSC in THF or toluene or without any solvent to form non-oxide gels which are practically free of any chlorine or oxygen and contain only small amounts of silicon. The composition of the polymer is relatively close to that of BCN<sub>2</sub>H<sub>2</sub> (Table 1). Powder XRD confirmed the amorphous state of this inorganic polymer.

The FT-IR and Raman spectra of the B/C/N xerogel clearly indicate the presence of N=C=N units showing characteristic asymmetric and symmetric C=N stretching modes around 2200 and 1600 cm<sup>-1</sup>, respectively (Figure 1).<sup>27</sup> The positions of these signals agree well with the data of molecular borylated carbodiimides of the type:<sup>28,29,30</sup>



Besides, the typical absorptions for N–H groups are found at 3440 cm<sup>-1</sup> as expected because of the hydrogen-

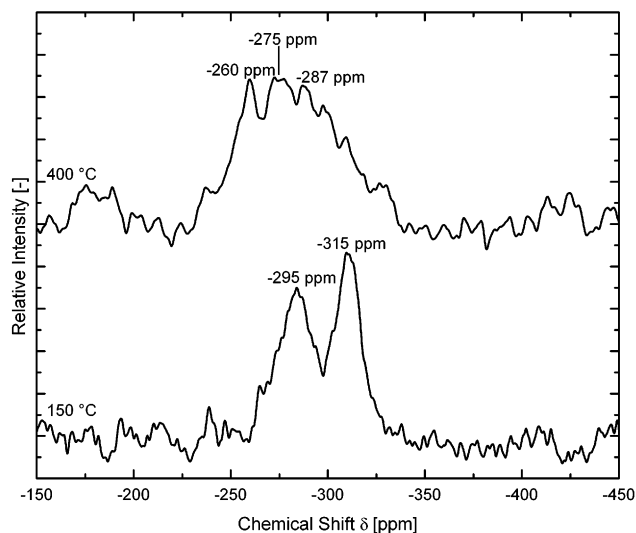


**Figure 2.**  $^{15}\text{N}$  CP MAS NMR spectra of the gel, dried in a vacuum at  $150\text{ }^\circ\text{C}$  and after calcination at  $400\text{ }^\circ\text{C}$  (contact time 3 ms, recycle delay 5 s, NS = 3600).

terminated borazene rings. An IR absorption band at  $2964\text{ cm}^{-1}$  and the corresponding Raman emission maxima at  $2964$  and  $2900\text{ cm}^{-1}$  show that residual Si-CH<sub>3</sub> groups are present. The signals at  $1402\text{ cm}^{-1}$  are most likely due to B-N valence vibrations, whereas the sharp emission band at  $862\text{ cm}^{-1}$  in the Raman spectrum is caused by a ring breathing vibration of the borazene rings.<sup>31</sup> N-Si vibrations of Si(CH<sub>3</sub>)<sub>3</sub> endgroups are probably responsible for the absorption at  $1080\text{ cm}^{-1}$  in the IR spectrum. However, the above-mentioned elemental analysis proves that the xerogel contains only a minor amount of silicon, indicating that the number of Si(CH<sub>3</sub>)<sub>3</sub> units in the network structure is relatively small.

To support this interpretation of the vibrational spectra and to gain further information about the polymer structure, solid-state NMR experiments were performed. The  $^{15}\text{N}$  CP MAS NMR spectrum (Figure 2) shows two peaks at  $-295$  and  $-315$  ppm. IRCP experiments were used to assess the degree of protonation of these sites (Figure 3). The signal at  $-295$  ppm exhibits a behavior characteristic of a NH group. Considering its chemical shift value it can be assigned to the NH units of a borazene ring, i.e., to a B<sub>2</sub>NH environment. The signal at  $-315$  ppm, with a very slow inversion rate, corresponds to a nonprotonated nitrogen site. Regarding the carbodiimide  $^{15}\text{N}$  chemical shift value observed in poly(methylsilsesquicarbodiimide), [CH<sub>3</sub>Si(NCN)<sub>1.5</sub>]<sub>n</sub>, which was found at  $-323$  ppm,<sup>17</sup> this signal can be attributed to a 2-fold coordinated nitrogen in a B-N=C=N-B environment. The  $^{11}\text{B}$  MAS NMR spectrum of

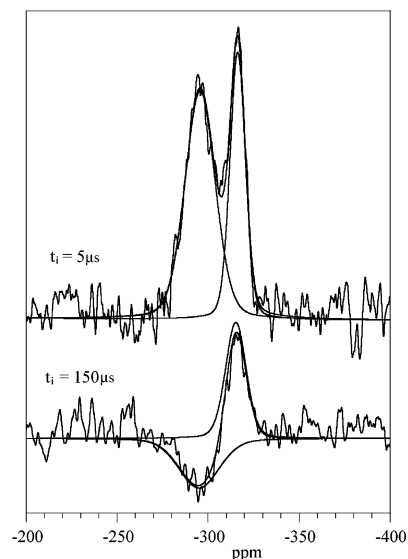


**Figure 3.**  $^{15}\text{N}$  IRCP MAS NMR spectra recorded on the BCN<sub>2</sub>H<sub>2</sub> xerogel for two inversion time values (contact time 3 ms, recycle delay 5 s, NS = 3600).

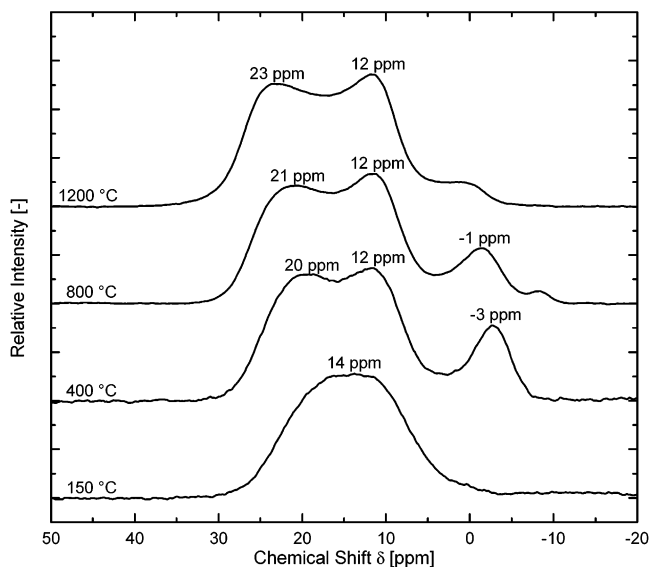


**Figure 4.**  $^{11}\text{B}$  MAS NMR spectra of the BCN<sub>2</sub>H<sub>2</sub> polymer xerogel, and pyrolysis products obtained at different temperatures (recycle delay 1 s, pulse angle  $\approx 20^\circ$ , NS = 160).

the polymer (Figure 4) shows a signal that is characteristic for a 3-fold coordinated boron atom in a BN<sub>3</sub> site as observed, for instance, in *h*-BN ( $\delta \approx 30$  ppm,  $C_Q \approx 2.8$  MHz,  $\eta \approx 0$ ).<sup>32</sup>

On the basis of the XRD data, spectroscopic results, and elemental analysis we propose an idealized polymer structure, which is illustrated in Scheme 1. Borazene rings are connected via carbodiimide groups forming a three-dimensional network which is free of chlorine atoms containing a small number of trimethylsilyl endgroups. Because of the limited sensitivity and resolution of NMR and vibrational spectra it cannot be completely excluded that a small amount of cyanamid units (N-C≡N) is also present in the xerogel.

**3.2 Polymer to Amorphous Ceramic Conversion.** The BCN<sub>2</sub>H<sub>2</sub> xerogel was pyrolyzed in dry argon at

(26) Nicolich, J. Dissertation, Darmstadt University of Technology, Germany, 2000 (in German). (b) Ruwisch, L. Dissertation, Darmstadt University of Technology, Germany, 1998 (in German).

(27) Weidlein, J.; Müller, U.; Dehnicke, K. *Schwingungsspektroskopie* Thieme Stuttgart, 2. Aufl., 1988.

(28) Einholz, W.; Haubold, W. *Z. Naturforsch.* **1986**, *41b*, 1367. (b) Sawitzki, G.; Einholz, W.; Haubold, W., *Z. Naturforsch.* **1988**, *43b*, 1179.

(29) Arthur, M.-P.; Goodwin, H. P.; Baccaredo, A.; Dillon, K. B.; Bertrand, G.; *Organometallics* **1991**, *10*, 3205.

(30) Geisberger, G.; Neukirchinger, K.; Nöth, H. *Chem. Ber.* **1990**, *123*, 455.

(31) Jones, T. B.; Maier, J. P.; Marthaler, O. *Inorg. Chem.* **1979**, *18*, 2140.

(32) Marchetti, P. S.; Kwon, D.; Schmidt, W. R.; Interrante, L. V.; Maciel, G. E. *Chem. Mater.* **1991**, *3*, 482.

Scheme 1

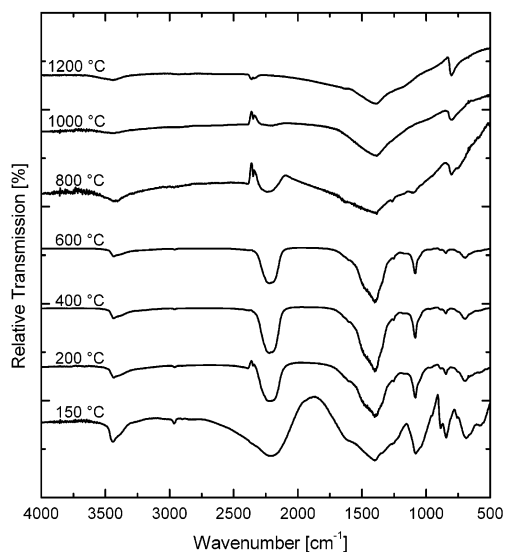
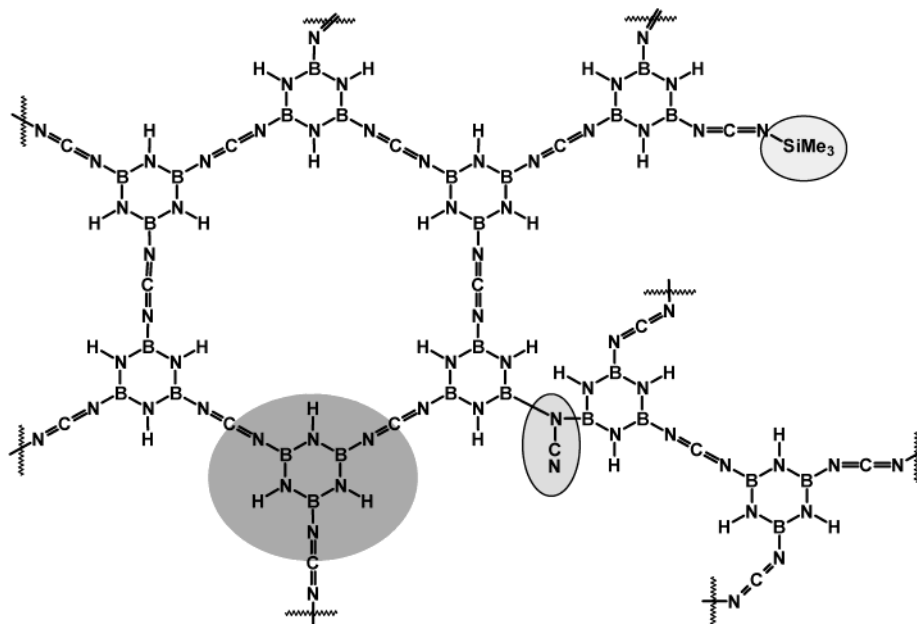


**Figure 5.** FT-IR spectra of the B/C/N(H) materials formed by heat treatment of the xerogel between 150 °C and 1200 °C.

different temperatures using a heating rate of 100 K/h. The FT-IR spectra of the samples synthesized between 150 °C and 1200 °C indicate structural changes of the network structure (Figure 5). Up to 800 °C the characteristic signals for the carbodiimide and the N–H groups are detectable. Between 800 °C and 1000 °C the N=C=N unit decomposes and the hydrogen content is decreased. An absorption band around 1400 cm<sup>-1</sup> caused by B–N valence vibrations is found in all spectra in Figure 5. Interestingly, this band sharpens in the temperature range from 150 to 600 °C and becomes very broad again between 600 and 800 °C. The signal at 1080 cm<sup>-1</sup>, which was attributed to Si–N vibrations (see above), disappears in the latter temperature region. A peak around 800 cm<sup>-1</sup> for the samples obtained at 800 to 1200 °C is probably due to a B–C stretching mode.<sup>33</sup>

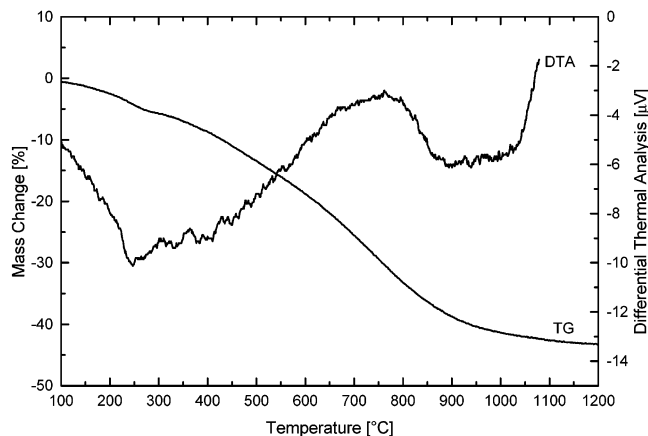


**Figure 6.** TGA and DTA curves for the BCN<sub>2</sub>H<sub>2</sub> xerogel.

According to a TGA–MS investigation a continuous ceramization process occurs in the temperature range up to 1200 °C (Figure 6). This was frequently observed for boron containing polymeric precursors including other B/C/N<sup>26a</sup> and Si/B/C/N<sup>14,26b</sup> materials. From 200 to 400 °C ammonia, as well as minor amounts of carbon-containing species are evolved causing a mass loss of ~5%. Larger amounts of methane and ammonia are formed between 400 and 1100 °C resulting in another mass loss of ~40%. This corresponds well with the elemental analysis data which show a strong decrease of the carbon and hydrogen contents for the product obtained at 1200 °C as compared to the xerogel (see Table 1).

The <sup>15</sup>N CP MAS NMR spectrum of the polymer heat-treated at 400 °C (Figure 2) shows a broad signal from –240 to –330 ppm indicating changes in the nitrogen environments. Many sites such as NB<sub>3</sub>, NHB<sub>2</sub>, NCB<sub>2</sub>, NBC<sub>2</sub>, and NCBH have already been observed in this chemical shift region.<sup>34</sup> Unfortunately, the poor signal-to-noise ratio of the spectrum due to the small amount of protons prevents determination of the number of individual components constituting this large signal. For

(33) Lanzisera, D. V.; Andrews, L.; Taylor, P. R. *J. Phys. Chem. A* **1997**, *101*, 7134.

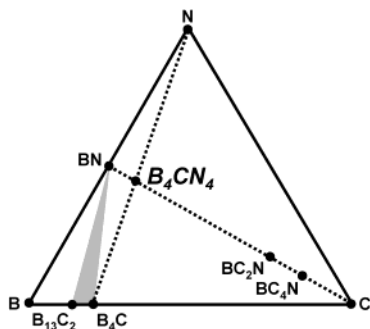


**Figure 7.** B/C/N ternary compositional diagram showing several known phases and the pyrolysis product obtained at 1200 °C. This phase has an elemental composition very close to  $B_4CN_4$  which is located on the C–BN as well as the N– $B_4C$  tie-lines. Therefore, it may be transformed to graphitic and/or diamond-like crystalline phases. At 2000 °C  $N_2$  is evolved and  $B_4C$  is formed.

the same reason, i.e., a lack of significant amounts of hydrogen in the samples, no signal could be detected for the materials pyrolyzed at >600 °C.

All  $^{11}B$  MAS NMR spectra of pyrolysis products obtained at temperatures up to 1200 °C (Figure 4) show the signal characteristic of  $BN_3$  environments which was also observed for the polymer. No signal corresponding to  $BCN_2$  sites ( $\delta \approx 37$  ppm)<sup>34(c)</sup> is detectable. An additional narrow signal is found around –4 ppm which most likely corresponds to 4-fold coordinated boron atoms.

The pyrolysis product formed at 1200 °C was analyzed for its carbon, hydrogen, boron, chlorine, silicon, and oxygen contents (Table 1). Only very minor amounts of oxygen and hydrogen are present and the silicon content is also relatively small. The exact elemental composition of  $BC_{0.23}N_{1.1}Si_{0.05}H_{0.09}O_{0.03}$  can approximately be described by the stoichiometric formula  $B_4CN_4$ , which is remarkable (Figure 7). In the literature mainly carbon-rich  $B_xC_yN_z$  ternary phases with  $y > x, z$  have been reported, especially when  $x = z$  (see below).

X-ray powder diffraction with the 1200 °C pyrolysis product indicated that this material is amorphous. A very broad and weak (100) reflex for turbostratically disordered graphite-like structures is present around  $2\theta = 43^\circ$ . This is typical for amorphous B/C/N materials formed by polymer pyrolysis around 1000 to 1200 °C. These phases are metastable and do not change upon long-term annealing at the said temperatures.<sup>26a</sup> HR-TEM confirmed the XRD results by showing no crystalline regions and a featureless homogeneous structure.

The exact distribution of carbon, boron, and nitrogen in turbostratically disordered or amorphous B/C/N materials is very difficult to determine. From the vibrational spectra discussed above and the  $^{11}B$  NMR data we conclude that there are B/N-rich graphitic layers mixed with carbon rich regions. However, according to the results of electron microscopy the overall element distribution is very homogeneous justifying describing the 1200 °C pyrolysis product as a single-phase amorphous material.

Numerous publications on B/C/N materials have appeared in recent years. Various vapor phase deposition techniques were used to generate B/C/N coatings.<sup>1,2,35</sup> Alternative routes include pyrolytic ceramizations of polymeric precursors<sup>1,2,36</sup> and high temperature/high pressure<sup>37</sup> synthesis methods. In certain cases, the authors described their B/C/N products as true solid solutions, whereas in other cases boron nitride–carbon mixtures are formed. As the binary phases<sup>2,38</sup> of the B/C/N system c-BN and  $B_4C$ , the  $sp^3$ -hybridized ternary phases are characterized by extreme hardness and diamond-like properties.<sup>39</sup> Ternary  $B_xC_yN_z$  phases with  $x = z$  were most frequently investigated because B–N units are isoelectronic to C–C units providing the theoretical possibility designing “defect-free” B/C/N networks with diamond- as well as graphite-like structures. The compositions  $BC_2N$ <sup>35c,35e,36d,40,41</sup> and  $BC_4N$ <sup>35a,36d,42</sup> have been described by several authors.  $BC_4N$  is reported to be formed upon pyrolysis of pyridine borane,  $C_5H_5N \cdot BH_3$ , and CVD. Similarly,  $BC_2N$  was obtained by thermal ceramization of piperazine borane,  $C_4H_{10}N_2 \cdot BH_3$ , and CVD. Several theoretical studies have been focused on crystalline B/C/N phases of this composition.<sup>41</sup> Further  $BC_xN$  materials, e.g., a  $BC_3N$  phase,<sup>43</sup> have been described in the literature. However, to our knowledge no B/C/N material with a composition close to  $B_4CN_4$  has been reported.

Single-phase  $B_xC_yN_z$  materials with  $x = z$  are promising precursors for the high-pressure transformation to

(35) see e.g., (a) Hegemann, D.; Riedel, R.; Dreßler, W.; Oehr, C.; Schindler, B.; Brunner, H. *Chem. Vap. Deposition* **1997**, *3*, 257. (b) Maya, L.; Richards, H. L. *J. Am. Ceram. Soc.* **1991**, *74*, 406. (c) Popov, C.; Saito, K.; Ivanov, B.; Koga, Y.; Fujiwara, S.; Shanov, V. *Thin Solid Films* **1998**, *312*, 99. (d) Saugnac, F.; Teyssandier, F.; Marchand, A. *J. Am. Ceram. Soc.* **1992**, *75*, 161. (e) Watanabe, M. O.; Itoh, S.; Mizushima, K.; Sasaki, T. *Appl. Phys. Lett.* **1996**, *68*, 2962. (f) Ulrich, S.; Ehrhardt, H.; Theel, T.; Schwan, J.; Westermeyer, S.; Scheib, M. *Diamond Relat. Mater.* **1998**, *7*, 839. (g) Stanishevsky, A.; Li, H.; Badzian, A.; Badzian, T.; Drawl, W.; Khriachtchev, L.; McDaniel, E., *Thin Solid Films* **2001**, *398–399*, 270. (h) Mieno, M.; Satoh, T. *J. Mater. Sci.* **2001**, *36*, 3925. (i) Oliveira, M. N.; Conde, O. *J. Mater. Res.* **2001**, *16*, 734. (j) Polo, M. C.; Martinez, E.; Esteve, J.; Andujar, J. L. *Diamond Relat. Mater.* **1999**, *8*, 423. (k) Hegemann, D.; Riedel, R.; Oehr, C. *Thin Solid Films* **1999**, *339*, 154.

(36) see e.g., (a) Riedel, R.; Bill, J.; Kienzle, A. *Appl. Organomet. Chem.* **1996**, *10*, 241. (b) Seyferth, D.; Rees, W. S., Jr. *Chem. Mater.* **1991**, *3*, 1106. (c) Maya, L. *J. Am. Ceram. Soc.* **1988**, *71*, 1104. (d) Bill, J.; Frieß, M.; Riedel, R., *Eur. J. Solid State Inorg. Chem.* **1992**, *29*, 195. (e) Komatsu, T.; Goto, A. *J. Mater. Chem.* **2002**, *12*, 1288. (f) Sauter, D.; Schempp, S.; Weinmann, M.; Muller, A.; Bill, J.; Lamparter, P.; Aldinger, F. *Mater. Res. Soc. Symp. Proc.* **1999**, *576*, 39. (g) Andreev, Y. G.; Lundström, T.; Harris, R. K.; Oh, S.-W.; Apperley, D. C.; Thompson, D. P. *J. Alloys Compounds* **1995**, *227*, 102.

(37) See e.g., (a) Paisley, M.; Horie, Y.; Davis, R. F.; Dan, K.; Tamura, H.; Sawaoka, A. B. *J. Mater. Sci. Lett.* **1993**, *12*, 1447. (b) Knittle, E.; Kaner, R. B.; Jeanloz, R.; Cohen, M. L. *J. Electron Microsc.* **1996**, *45*, 135. (c) Yamada, K. *J. Am. Ceram. Soc.* **1998**, *81*, 1941.

(38) Kulisch, W. *Phys. Status Solidi. A* **2000**, *177*, 63. (39) Lundström, T.; Andreev, Y. G. *Mater. Sci. Eng. A* **1996**, *209*, 16.

(40) For experimental work on  $BC_2N$  see e.g., (a) Sasaki, T.; Akaishi, M.; Yamaoka, S.; Fujiki, Y.; Oikawa, T. *Chem. Mater.* **1993**, *5*, 695. (b) Nakano, S.; Akaishi, M.; Sasaki, T.; Yamaoka, S. *Chem. Mater.* **1994**, *6*, 2246. (c) Kagi, H.; Tsuchida, I.; Masuda, Y.; Okuda, M.; Katsura, K.; Wakatsuki, M. *High Pr. Sci. Technol.* **1996**, *258*.

(41) For theoretical work on  $BC_2N$  phases see (a) Liu, A. Y.; Wentzcovitch, R. M.; Cohen, M. L. *Phys. Rev. B* **1989**, *39*, 1760. (b) Widany, J.; Verwoerd, W. S.; Frauenheim, T. *Diamond Relat. Mater.* **1998**, *7*, 1633. (c) Nozaki, H.; Itoh, S. *J. Phys. Chem. Solids* **1996**, *57*, 41. (d) Tateyama, Y.; Ogitsu, T.; Kusakabe, K.; Tsuneyuki, S.; Itoh, S. *Phys. Rev. B* **1997**, *55*, R10161. (e) Mattesini, M.; Matar, S. F. *Int. J. Inorg. Mater.* **2001**, *3*, 943.

(42) Walker, B. E., Jr.; Rice, R. W.; Becher, P. F.; Bender, B. A.; Coblenz, W. S. *Ceram. Bull.* **1983**, *62*, 916. (b) Solozhenko, V. L.; Turkevich, V. Z.; Sato, T. *J. Am. Ceram. Soc.* **1997**, *80*, 3229.

(43) Kawaguchi, M.; Kawashima, T. *J. Chem. Soc., Chem. Commun.* **1993**, 1133.

(34) Gervais, C.; Maquet, J.; Babonneau, F.; Duriez, C.; Framery, E.; Vaultier, M.; Florian, P.; Massiot, D. *Chem. Mater.* **2001**, *13*, 1700. (b) Franz, T.; Hanecker, E.; Nöth, H.; Stöcker, W.; Storch, W.; Winter, G. *Chem. Ber.* **1986**, *119*, 900. (c) Nöth, H.; Wrackmeyer, B. *Chem. Ber.* **1974**, *107*, 3089. (d) Cornu, D.; Miele, P.; Faure, R.; Bonnetot, B.; Mongeot, H.; Bouix, J. *J. Mater. Chem.* **1999**, *9*, 757.

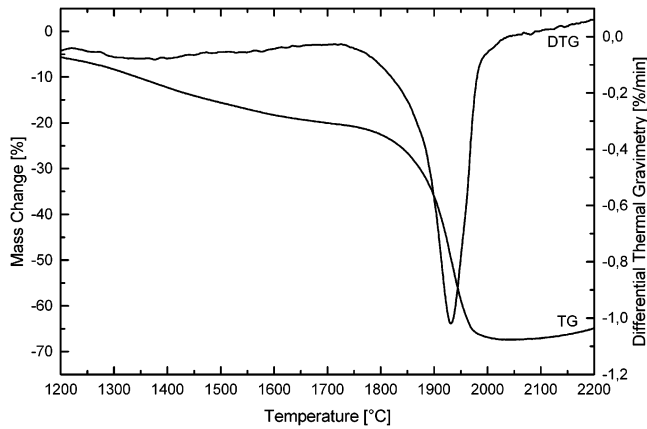


**Figure 8.** Thermal analysis (TGA and DTG) of the amorphous B<sub>4</sub>CN<sub>4</sub> material between 1200 °C and 2200 °C.

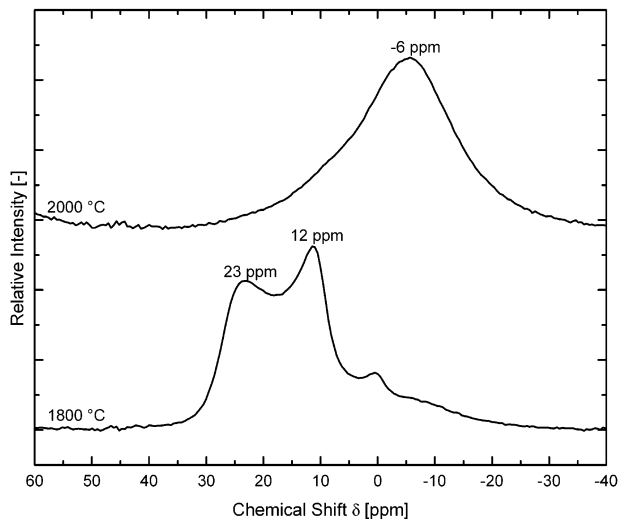


**Figure 9.** <sup>11</sup>B-MAS NMR spectra obtained for the sol-gel derived B/C/N materials annealed at 1800 °C and 2000 °C (recycle delay 1 s, pulse angle ≈20°, NS = 160).

crystalline sp<sup>3</sup>-hybridized structures. Especially methods which are capable to generate very high pressures and temperatures such as laser-heated diamond anvil cells, multi-anvil presses, or shock synthesis methods,<sup>44</sup> may be used to prepare a novel crystalline B<sub>4</sub>CN<sub>4</sub> phase. Very recently, this has successfully been demonstrated for hexagonal<sup>45</sup> as well as cubic<sup>46</sup> BC<sub>2</sub>N structures.

The new phase B<sub>4</sub>CN<sub>4</sub> not only lies on the BN–C tie-line but also on the B<sub>4</sub>C–N, as shown in Figure 7. Therefore, this composition offers the opportunity to generate boron carbide upon high-temperature annealing.

**3.3 Characterization of the Crystallization Process.** Further annealing of the amorphous B/C/N phase obtained at 1200 °C was investigated by TGA–MS as illustrated in Figure 8. Between 1200 and 1800 °C the material exhibits a mass loss of about 15% which is due to the formation of nitrogen and small amounts of volatile silicon-containing species. A major mass loss of ~45% at 1850 to 1975 °C is caused by the decomposition of the B<sub>4</sub>CN<sub>4</sub> phase forming two equivalents of N<sub>2</sub> and

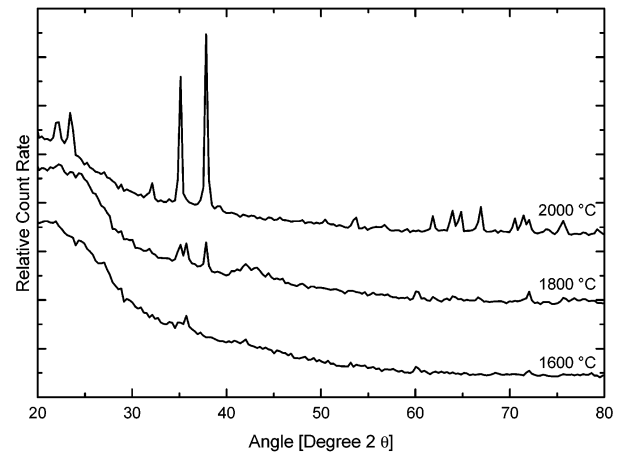


**Figure 10.** XRD patterns of B/C/N materials annealed at the designated temperatures under inert gas.

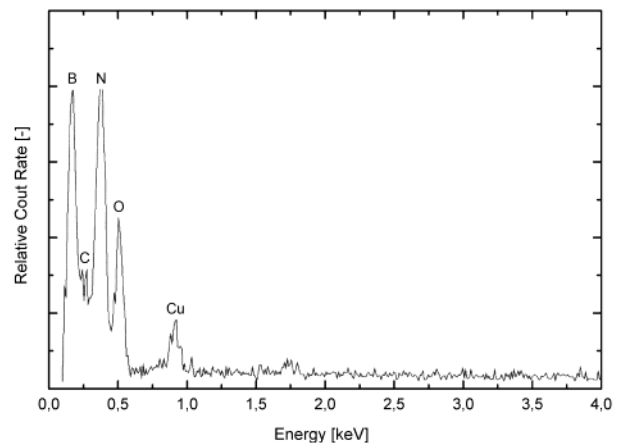
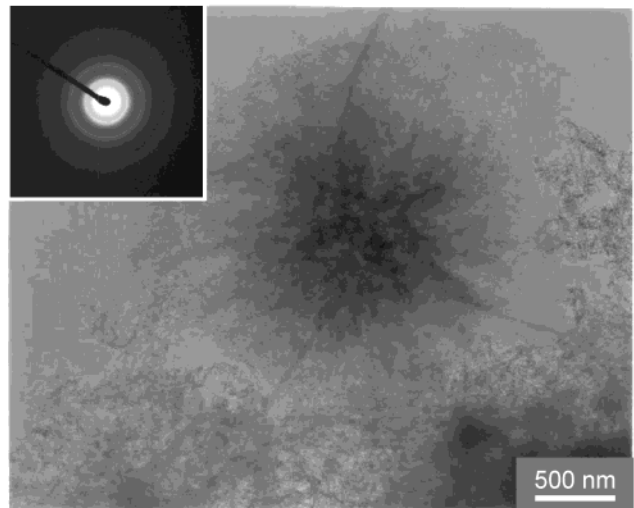


**Figure 11.** (a) TEM image and SAED pattern of an amorphous region of the material obtained at 1800 °C. (b) EDX analysis of the same part of the sample.

B<sub>4</sub>C. Again, these results correspond well with the elemental analysis (see Table 1).

FTIR spectra of samples annealed at 1400, 1600, and 1800 °C indicate no significant changes compared to the spectrum of the B<sub>4</sub>CN<sub>4</sub> material obtained at 1200 °C showing an intense absorption band around 1300 cm<sup>-1</sup>. This band completely disappears at 2000 °C resulting in a featureless spectrum without any peaks in the standard IR region between 500 and 4000 cm<sup>-1</sup> as it was reported for B<sub>4</sub>C.<sup>47</sup>

(44) Overview: Kroke, E. *Angew. Chem., Int. Ed.* **2002**, *41*, 77.

(45) Nicolich, J. P.; Hofer, F.; Brey, G.; Riedel, R. *J. Am. Ceram. Soc.* **2001**, *84*, 279.

(46) Solozhenko, V. L.; Andrault, D.; Fiquet, G.; Mezouar, M.; Rubie, D. C. *Appl. Phys. Lett.* **2001**, *78*, 1385.

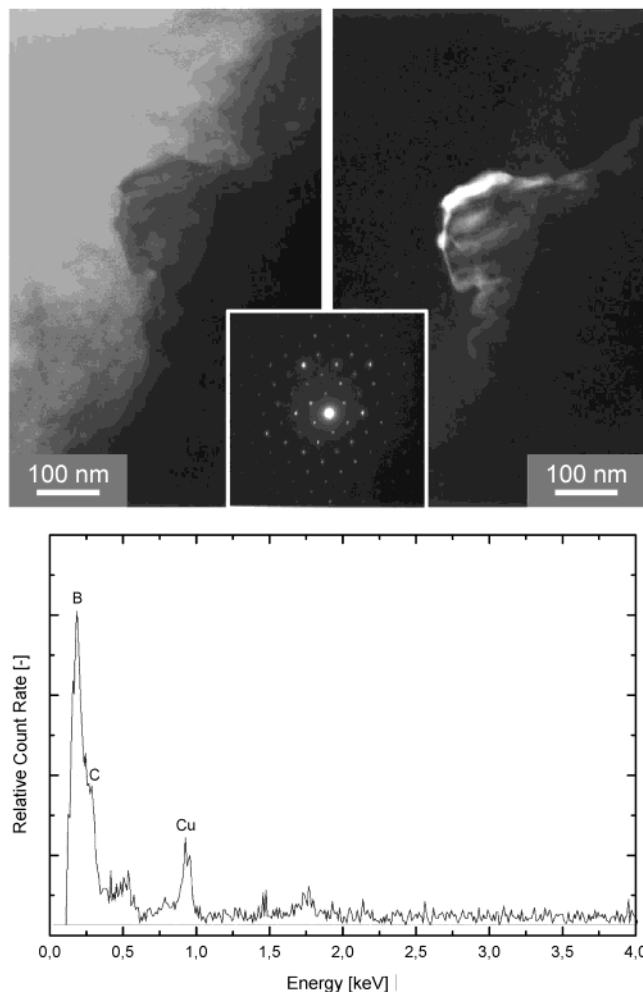


**Figure 12.** Transmission electron microscopy studies on the material formed upon pyrolysis under argon at 1800 °C for 4 h. (a) Dark and bright field image of a microcrystalline region of the sample with an electron diffraction pattern in the center which was analyzed to correspond to the [110] of rhombohedral B<sub>4</sub>C. (b) EDX analysis of the same part of the sample.

Similarly, <sup>11</sup>B-MAS NMR spectra of the samples pyrolyzed at temperatures ranging from 1200 to 1800 °C are practically identical (compare Figures 4 and 9). The main signal ( $\delta = 28$  ppm,  $C_Q = 2.8$  MHz,  $\eta = 0$ ) is characteristic for the BN<sub>3</sub> sites of borazene rings typically found in hexagonal boron nitride. The spectrum of the material annealed at 2000 °C, however, is completely changed (Figure 9). It resembles the <sup>11</sup>B-MAS NMR spectrum of a commercial B<sub>4</sub>C sample<sup>48</sup> measured under the same conditions for comparison.

XRD investigation showed that the material synthesized at 1600 °C is still amorphous (Figure 10). Interestingly, the broad signal around  $2\theta = 43^\circ$  which indicates turbostratically disordered B/C/N phases cannot be detected, in contrast to the above-described material formed at 1200 °C. The product obtained at 1800 °C has started to crystallize as indicated by the appearance of relatively sharp but weak reflections which are at least in part due to rhombohedral boron carbide. An XRD

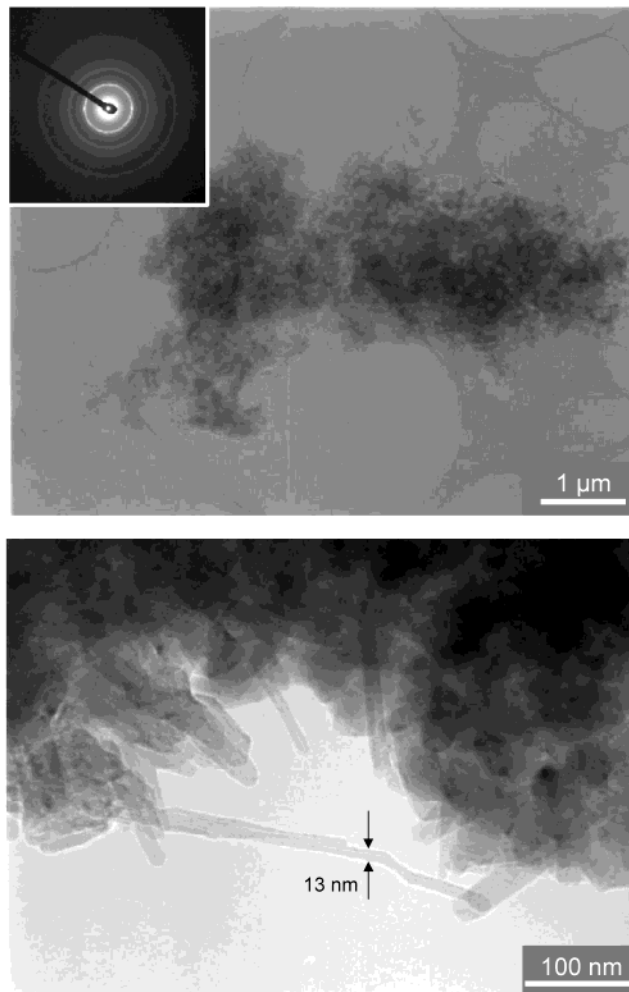


**Figure 13.** TEM image of an amorphous region of the sample obtained after annealing at 2000 °C for 4 h. (b) Higher magnification of the amorphous part indicating the formation of multiwalled carbon nanotubes. EDX analysis for this region of the sample indicated the absence of elements other than carbon.

pattern with sharp signals is found for the sample annealed at 2000 °C which shows all the reflections expected for rhombohedral B<sub>4</sub>C according to the PDF database.<sup>49</sup> No additional signals for crystalline phases are found.

HR-TEM studies on the microstructure of the product heat-treated at 1800 °C revealed that the main fraction of the sample is amorphous, as shown in Figure 11. EDX analysis indicates the presence of boron, carbon, nitrogen, and oxygen. Boron and nitrogen are the major components with a B/N ratio close to 1:1. Very few microcrystalline particles were also detected which were identified by SAED as boron carbide (Figure 12). EDX analysis of the crystallites indicates a B/C ratio of approximately 4:1. The material obtained upon pyrolysis at 2000 °C for 4 h consists primarily of crystalline boron carbide with crystallite sizes in the range of 0.5 to 3 μm (see below) as expected from the spectroscopic and elemental analysis data. However, a very small amount of amorphous graphite-like carbon was also found (Figure 13). Part of these amorphous regions contained

(47) SDBSWeb Database. National Institute of Advanced Industrial Science and Technology, Tsukuba, Ibaraki, Japan; <http://www.aist.go.jp/RIODB/SDBS/>; (accessed May 21, 2002).

(48) Simeone, D.; Mallet, C.; Dubuisson, P.; Baldinozzi, G.; Gervais, C.; Maquet, J. *J. Nuclear Mater.* **2000**, *227*, 1.

(49) Powder Diffraction Files (PDF), International Center for Diffraction Data: Swarthmore, PA.



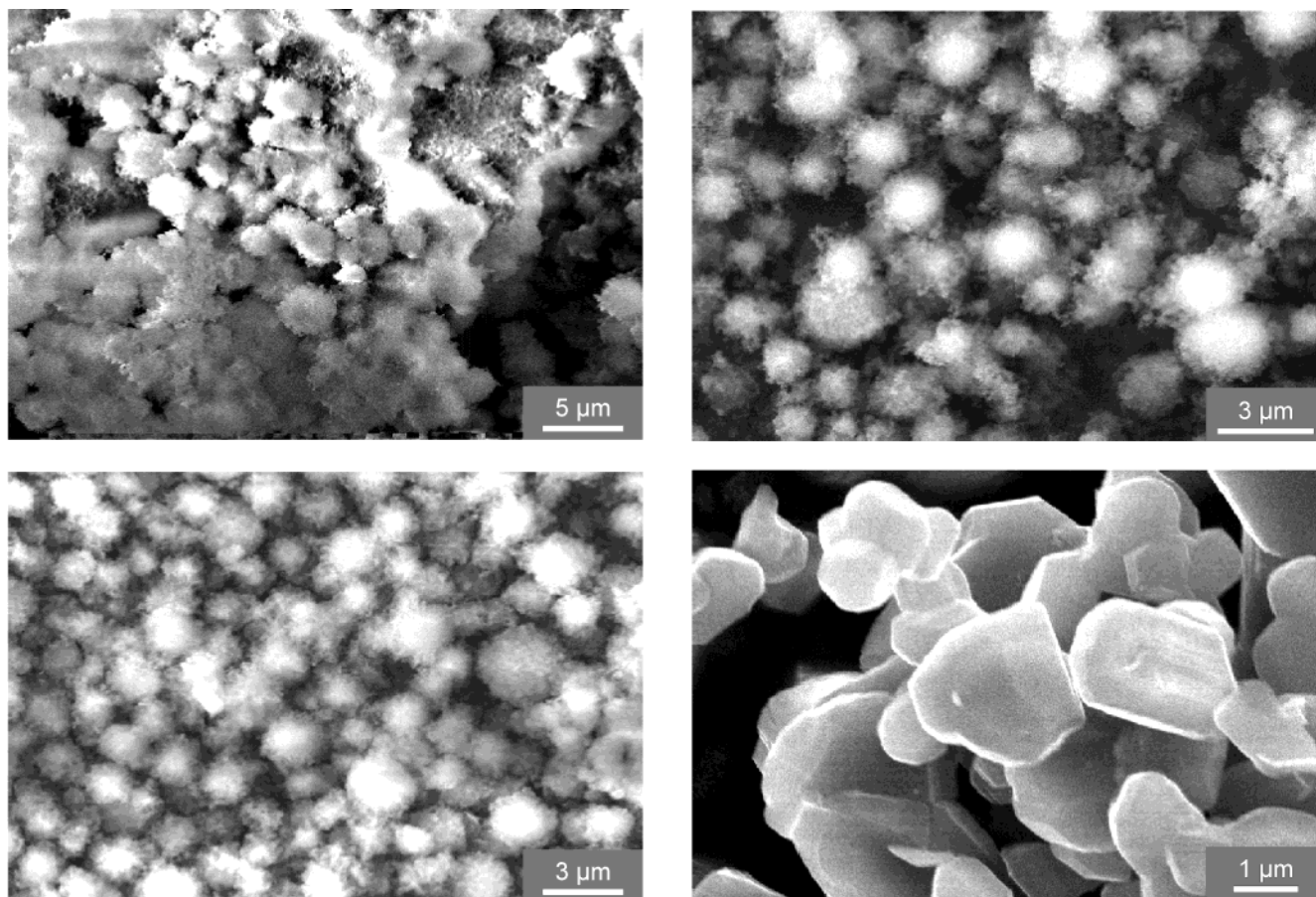


**Figure 14.** SEM images of the B/C/N gel (a) after drying in a vacuum at 150 °C, (b) after annealing at 1200 °C, (c) after heat treatment at 1800 °C, and (d) after crystallization at 2000 °C.

multiwalled carbon nanotubes. The only element which was detectable by EDX analysis is carbon. Because of the limited sensitivity of EDX analysis it cannot be completely excluded that the nanotubes as well as the other parts of the amorphous regions might contain small amounts of boron and/or nitrogen. No efforts were made to investigate the structure of the nanotubes in detail, e.g. with EELS, because of the small yield. Boron-doped multiwalled carbon nanotubes and B/C/N nanotubes have been prepared by the arc-discharge method using boron-containing graphite electrodes as well as the CVD method.<sup>50</sup> Also, the formation of carbon nanotubes by solid-state pyrolysis has been reported.<sup>51</sup>

**3.4 Morphological Characterization and Possible Applications.** It should be pointed out that the phenomenology of the sol–gel transition observed for the borazene-carbodiimide system presented here is very similar to typical oxide sol–gel processes. As it was examined in detail for poly(silylcarbodiimide) gels, a homogeneous and transparent liquid reaction mixture solidifies – after a reaction time of typically 0.5 to 100 hours – within minutes to form a shape-retaining gel

body, which is sometimes transparent for visible light.<sup>16–23</sup>

The morphology of the xerogels and the pyrolysis products were investigated using scanning electron microscopy. The image in Figure 14a shows that the xerogel consists of porous (fractal) spherical particles with diameters of approximately 0.5–3 μm which are interconnected. A dendritic growth mechanism is most likely responsible for this observation. Surprisingly, the morphology does not change significantly upon pyrolysis at temperatures as high as 1800 °C as shown in Figure 14b and c. In contrast, a completely different morphology is found for the material annealed at 2000 °C, which exhibits agglomerated crystallites of 1–3-μm diameter (Figure 14d).

Nitrogen adsorption measurements analyzed according to the Brunauer–Emmett–Teller (BET) model indicate that the xerogel has a surface area of 85 m<sup>2</sup>/g. This is similar to the results of Paine and Narula et al. who found a value of 35 m<sup>2</sup>/g for their B/C/N xerogels,<sup>7</sup> and the BET surface areas measured for poly(silsesquicarbodiimide)-derived xerogels.<sup>17,18</sup> It is significantly less than the values of 500–1000 m<sup>2</sup>/g reported for the Si–N xerogel of Bradley et al.,<sup>6</sup> and that of many porous oxide xerogels. The small surface areas of the B/C/N xerogels may be related to the relatively large particle size of 0.5–3 μm as described above. Microporosity within the particles is obviously at least in part destroyed during drying of the gel by evacuation and heating. It is expected that much higher surface areas

(50) See e.g. (a) Terrones, M.; Benito, A. M.; Manteca-Diego, C.; Hsu, W. K.; Osman, O. I.; Hare, J. P.; Reid, D. G.; Terrones, H.; Cheetham, A. K. *Chem. Phys. Lett.* **1996**, *257*, 576. (b) Hsu, W. K.; Nakajima, T. *Carbon* **2002**, *40*, 462. (d) Suenaga, K.; Colliex, C.; Demoncy, N.; Loiseau, A.; Pascard, H.; Willaime, F. *Science* **1997**, *278*, 653. (e) Redlich, P.; Loeffler, J.; Ajayan, P. M.; Bill, J.; Aldinger, F.; Rühle, M. *Chem. Phys. Lett.* **1996**, *260*, 465. (f) Zhang, Y.; Gu, H.; Suenaga, K.; Iijima, S. *Chem. Phys. Lett.* **1997**, *279*, 264.

(51) Review: Journet, C.; Bernier, P. *Appl. Phys. A: Mater. Sci. Process.* **1998**, *A67*, 1.

will be obtained after careful supercritical drying or freeze-drying of the gels in order to form B/C/N aerogels.

Especially because of the attractive properties of B/C/N materials and boron carbide, the non-oxide sol-gel system presented here offers a number of potential applications and future areas of research. These include the generation of coatings and possibly fibers. The use of templates is well-known from the preparation of porous oxides and may open a route to micro-, meso-, and macro-porous B/C/N materials. Membranes and nanopowders may be produced as it was demonstrated for polysilylcarbodiimide gels. Furthermore, other elements or components, e.g., metal compounds or metal particles, can be introduced into the gels providing the opportunity to fabricate a wide range of hybrid and composite materials.

#### 4. Conclusion

Here we reported on a carbodiimide based sol-gel synthesis of B/C/N/(H) materials. The products obtained by drying are almost free of oxygen, chlorine, and silicon. Pyrolysis between 150 and 800 °C provides materials

that contain borazene rings connected by carbodiimide units. The amount of the latter decreases continuously with increasing temperature. At 1200 °C a novel amorphous  $B_4CN_4$  phase is formed, which is stable up to 1600 °C where it starts to crystallize. This novel nitrogen-rich  $B_4CN_4$  phase may be a promising amorphous precursor for high-pressure synthesis of crystalline B/C/N phases. Annealing at 2000 °C furnishes nearly pure  $B_4C$ , which is known for its extreme hardness and chemical inertness.

**Acknowledgment.** We gratefully acknowledge financial support from Deutsche Forschungsgemeinschaft (DFG, Bonn) through the project Kr1739/5-1 and the Fonds der Chemischen Industrie (FCI, Frankfurt). K.W.V. acknowledges a HSP III fellowship for Japan by the German Academic Exchange Service (DAAD), Bonn, Germany. E.K. is grateful to F. Lange (University of California, Santa Barbara, CA) for his support and to the Alexander von Humboldt-Foundation (Bonn) for granting a Feodor Lynen Fellowship.

CM021314J